

SUPPLEMENTARY FIGURE AND TABLES

Dynamic and structural constraints in signal propagation by regulatory networks

Javier Estrada¹ and Raúl Guantes¹

October 10, 2012

¹ Department of Condensed Matter Physics, Facultad de Ciencias, Universidad Autónoma de Madrid, Madrid, Spain, and Instituto 'Nicolás Cabrera', Facultad de Ciencias, Universidad Autónoma de Madrid, 28049 Madrid, Spain

Table S1: **Most correlated structural and dynamical features for 'AND' gates.** For each response property (main columns) and network topology(rows) we give the Spearman's coefficient of the most correlated structural/dynamical features. For comparison, we show both the most correlated feature (right columns) and the most correlated individual feature, either individual susceptibility or activation/deactivation time(left columns). All logic gates are of 'AND' type.

	Oscillations bandwidth				Propagated noise				Fluctuations bandwidth			
	structure		dynamics		structure		dynamics		structure		dynamics	
C1-FFL	S_{SI}	FS	T_{on}	ΣT	S_{OI}	S_O	T_{on}	ΔT	S_{SI}	S_{LC}	T_{on}	T_{on}
	0.50	1.00	-0.87	-0.99	0.61	0.99	0.64	-0.87	-0.70	-0.97	-0.89	-0.89
C3-FFL	S_{OI}	FS	T_{off}	ΣT	S_{SI}	S_O	T_{off}	ΔT	S_{SI}	S_{LC}	T_{off}	ΔT
	0.53	1.00	-0.87	-0.98	0.62	0.99	0.67	-0.95	-0.67	-0.96	-0.90	0.94
I1-FFL	S_{OS}	FS	T_{on}	ΣT	S_{OI}	S_O	T_{on}	ΔT	S_{SI}	FS	T_{on}	T_{on}
	0.48	1.00	-0.90	-0.97	0.89	0.97	0.67	-0.92	0.57	0.75	-0.82	-0.82
I3-FFL	S_{SI}	FS	T_{off}	ΣT	S_{OI}	S_O	T_{off}	ΔT	S_{SI}	FS	T_{off}	T_{off}
	0.44	1.00	-0.92	-0.98	0.90	0.96	0.69	-0.96	0.63	0.79	-0.82	-0.82
P-FB	S_{SO}	FS	T_{off}	ΣT	S_{OS}	S_O	T_{on}	T_{on}	S_{OS}	FS	T_{on}	ΣT
	0.39	1.00	-0.66	-0.92	0.78	0.99	0.16	0.16	-0.65	0.92	-0.55	-0.75
N-FB	S_{SO}	FS	T_{on}	ΣT	S_{SI}	S_{LC}	T_{off}	ΔT	S_{SO}	S_{SO}	T_{on}	T_{on}
	0.51	1.00	-0.96	-0.97	0.67	0.99	-0.32	-0.47	0.82	0.82	-0.58	-0.58

Table S2: **Most correlated structural and dynamical features for 'OR' gates.**

	Oscillations bandwidth				Propagated noise				Fluctuations bandwidth			
	structure		dynamics		structure		dynamics		structure		dynamics	
C1-FFL	S_{SI}	FS	T_{off}	ΣT	S_{OI}	S_O	T_{on}	T_{on}	S_{OS}	S_O	T_{on}	T_{on}
	-0.69	1.00	-0.90	-0.95	0.73	0.99	0.49	0.49	-0.70	-0.97	-0.65	-0.65
C3-FFL	S_{SI}	FS	T_{off}	ΣT	S_{OI}	S_O	T_{off}	ΔT	S_{OS}	S_O	T_{off}	ΔT
	-0.61	1.00	-0.91	-0.96	0.75	0.99	0.45	-0.69	-0.74	-0.97	-0.63	0.73
I1-FFL	S_{SI}	FS	T_{off}	ΣT	S_{OI}	S_O	T_{on}	T_{on}	S_{SI}	S_O	T_{on}	ΣT
	0.60	1.00	-0.92	-0.93	0.93	0.94	0.61	0.61	0.60	-0.69	-0.74	-0.75
I3-FFL	S_{SI}	FS	T_{off}	ΣT	S_{OI}	S_O	T_{off}	ΔT	S_{OI}	S_O	T_{off}	T_{off}
	0.50	1.00	-0.92	-0.94	0.93	0.96	0.44	-0.56	-0.58	-0.81	-0.67	-0.67
P-FB	S_{OS}	FS	T_{off}	ΣT	S_{OS}	S_O	T_{off}	ΣT	S_{OS}	FS	T_{on}	ΣT
	-0.56	1.00	-0.87	-0.98	0.66	0.99	0.48	0.54	-0.73	0.96	-0.86	-0.95
N-FB	S_{OS}	FS	T_{off}	ΣT	S_{SI}	S_{LC}	T_{off}	T_{off}	S_{SO}	S_{SO}	T_{off}	ΣT
	0.69	1.00	-0.92	-0.98	0.68	0.99	-0.51	-0.51	0.83	0.83	-0.66	-0.72

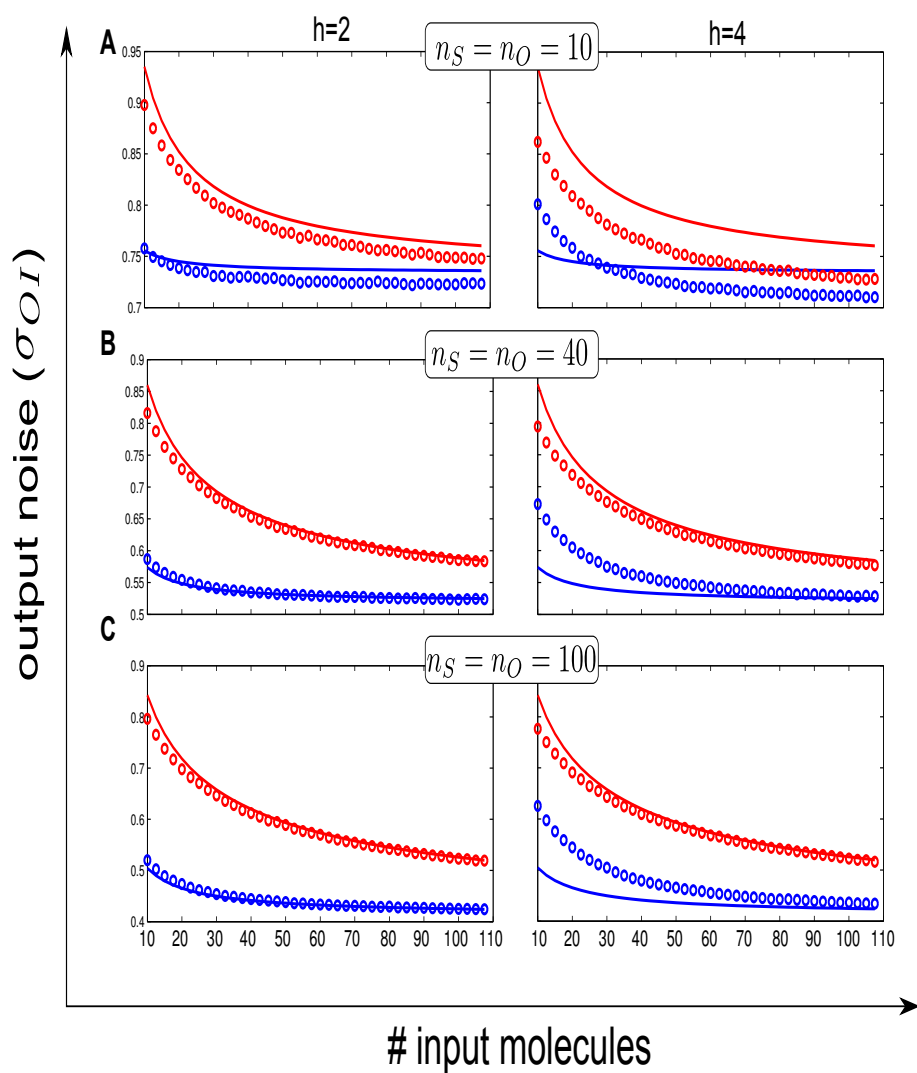


Fig. S1: The linear noise approximations (solid lines) is compared with MonteCarlo simulations (circles) for a C1-FFL (red) and an I1-FFL (blue) with 'AND' regulatory logic, see *Models of regulatory circuits* in *Methods*, main text. Two different Hill coefficients ($h = 2$, left panels, and $h = 4$, right panels) are used. Propagated noise is calculated varying the number of input molecules for different values of sensor and output copy numbers: $n_S = n_O = 10$ (top), $n_S = n_O = 40$ (middle) and $n_S = n_O = 100$ (bottom). In all cases susceptibilities are set to $s_{SI} = 1$, $s_{OS} = 2$, $s_{OI} = \pm 1.5$ and degradation rates for all components to $\delta_i = 1 \text{ h}^{-1}$.

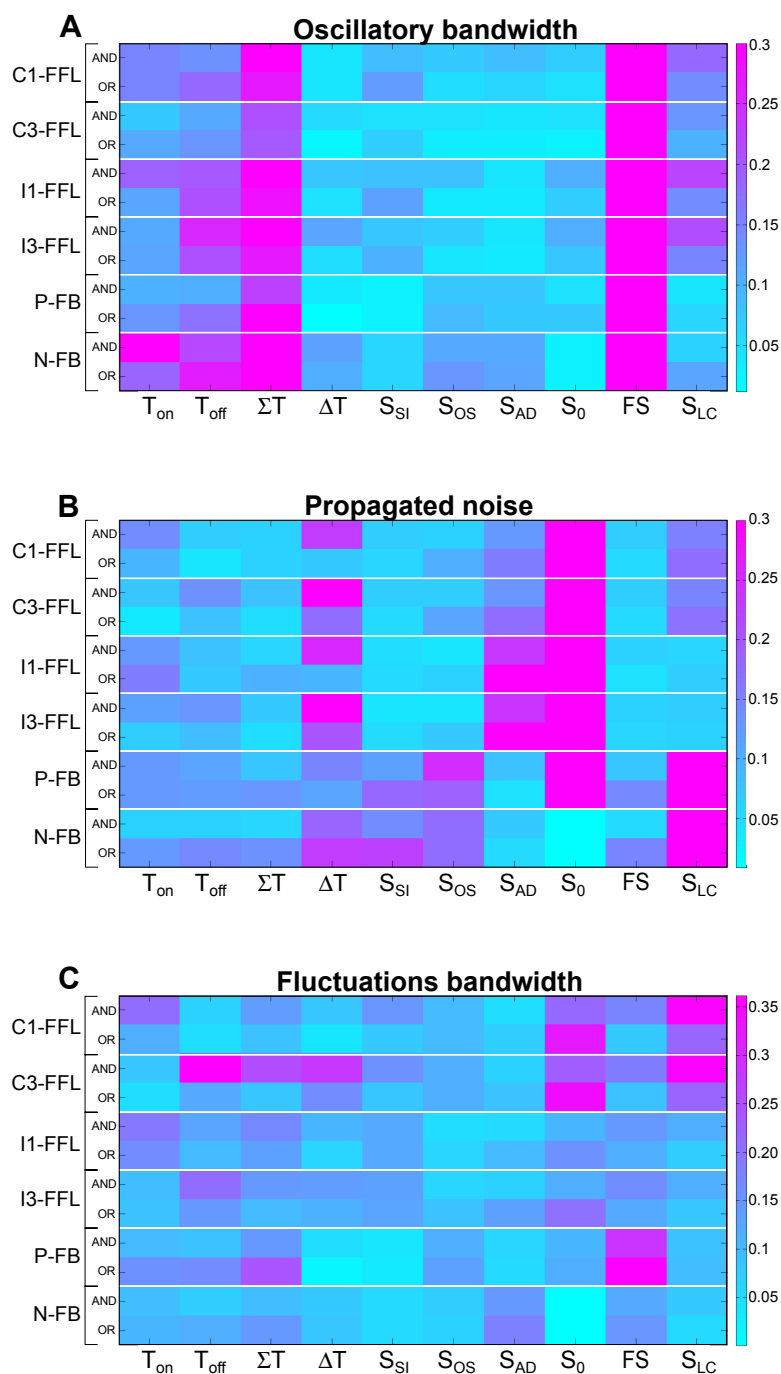


Fig. S2: Mutual information correlations between structural/dynamical features and responses. Color code values of the mutual information correlation coefficient between features and different network responses. A. Oscillatory bandwidth. B. Propagated noise. C. Bandwidth of fluctuation power spectra. As in Figure 5D-F, $s_{LC} = s_{OS} \cdot s_{SI}$ is the susceptibility of the linear cascade backbone of the circuits; s_{AD} represents the additional susceptibility: either s_{OI} for feedforward loops or s_{SO} for feedbacks.

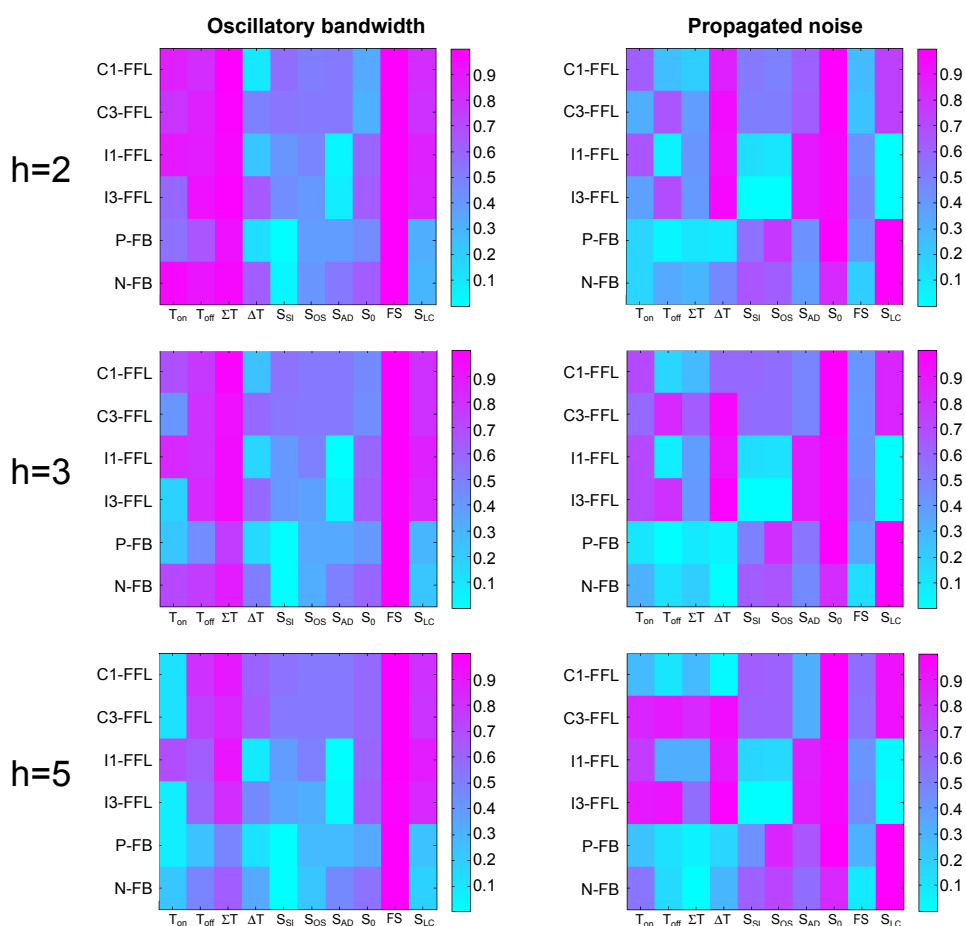


Fig. S3: **Effect of susceptibility ranges and Hill coefficients on correlations.** Spearman's rank correlations between the output responses and all the dynamical and structural features, computed for two different Hill coefficients ($h = 2, 3$ and 4) for circuits operating under 'AND' logic. 20,000 sets of random susceptibilities are generated, with susceptibilities $s_{ij} \in (0, h)$ and degradations $\delta_i = 1$.

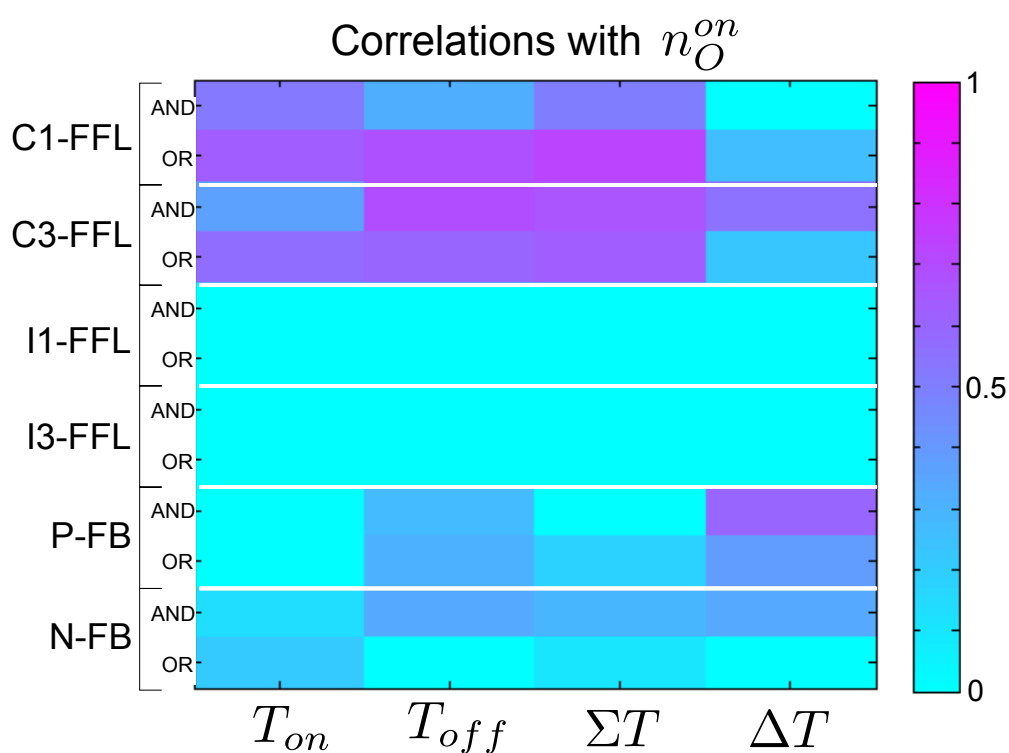


Fig. S4: **Response times are not sensitive to absolute changes in output.** Absolute value of Spearman's rank correlation between the different dynamical features and the final steady-state output concentration after the transient changes in input. 20,000 sets of random susceptibilities are generated with Hill coefficient $h = 2$, susceptibilities $s_{ij} \in (0, 2)$ and degradations $\delta_i = 1$. The poor correlations show that response times do not depend strongly on the changes in output.

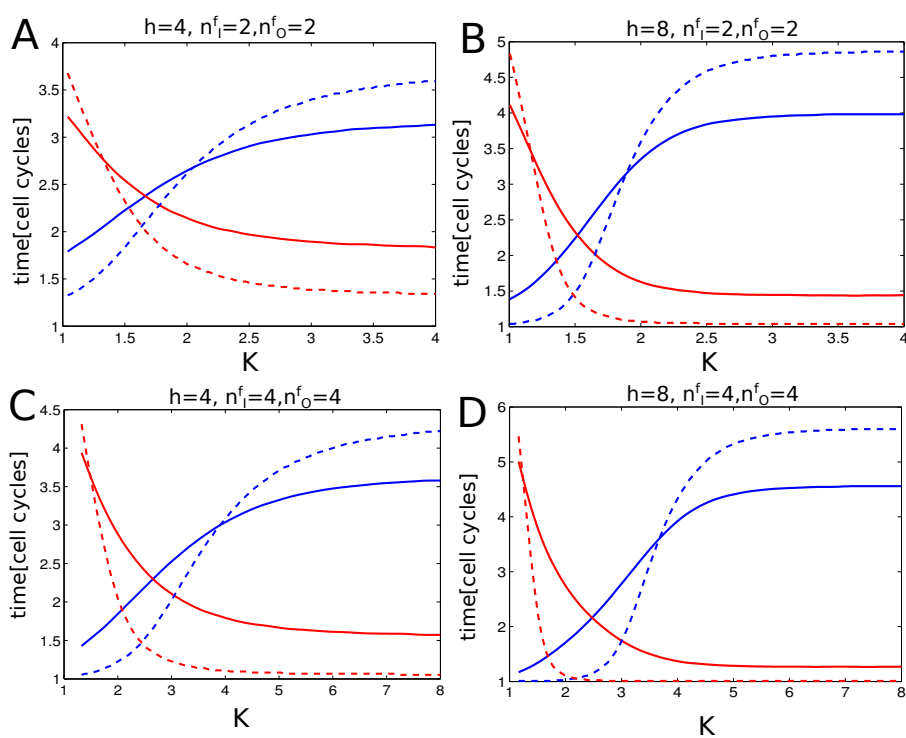


Fig. S5: **Effect of input/output levels and non-linearities on theoretical response times.** Numerical (solid lines) and theoretical (from Eq. (11) in main text, dashed lines) response times for a two-component cascade, Eq. (17) in main text, for different values of the Hill coefficient h and changes in input and output, as indicated in each panel (initial values are always $\bar{n}_I = \bar{n}_O = 1$). Activation times (T_{on}) are plotted in blue, deactivation times (T_{off}) in red. Compare to Figure 7 in main text.